KINETICS AND MECHANISM OF THE HYDROGEN-EVOLUTION REACTION ON MERCURY IN HCl–DIMETHYLSULPHOXIDE SOLUTIONS

D. POSADAS and A. J. ARVÍA

División Electroquímica, Instituto de Investigaciones Fisicoquímicas Teóricas y Aplicadas,
Facultad de Ciencias Exactas, Universidad Nacional de La Plata, La Plata, Argentina

Abstract—Rapid galvanostatic and potentiostatic stationary E/I curves, E/time characteristics at current interruption and electrode capacitance measurements were made to investigate hydrogen-ion discharge on mercury in HCl–DMSO solutions, with and without the addition of LiCl as supporting electrolyte. Kinetic parameters and their temperature and concentration dependences are discussed in terms of the initial electron-transfer reaction as rate-determining.

INTRODUCTION

The hydrogen-evolution reaction on mercury in aqueous solutions has been the subject of many publications, which have been compiled by Vetter[1], but the reaction in non-aqueous systems has not been investigated in such a way as to establish its reaction mechanism. There is a report about the polarographic wave of hydrogen discharge on the dme, from HCl dissolved in dimethylsulphoxide, where an estimation of the diffusion coefficient for the solvated hydrogen ion is made[2], and some publications on the hydrogen-electrode reaction in other solvents, such as acetonitrile and mixtures of acetonitrile and water[3, 4].

This reaction has been investigated in this laboratory using HCl–DMSO solutions on different metals, such as platinum[5, 6], iron[7] and nickel[8]. The reaction mechanism for these metals contains formally the reaction steps which have been discussed in detail for aqueous systems.

The present work comprises the study of HCl–DMSO solutions on Hg-pool and dropping Hg electrodes. These electrodes have been successfully employed in aqueous solutions[9]. LiCl was chosen as supporting electrolyte because of its high solubility and the existing physicochemical data on LiCl–DMSO solutions.

EXPERIMENTAL TECHNIQUE

A conventional three-compartment Pyrex-glass cell was used. The Hg-pool working electrode was replaced after each run to minimize the solution creeping at the Hg/glass interphase and Hg contamination[10]. The area of the electrode was 2·54 cm². An aqueous sce reference and a Pt counter-electrode were used.

DMSO (Baker a.r.) with a water content of 0·02 per cent was used as received and checked by the Karl Fischer method. LiCl (Merck, a.r.) was dried under vacuum before use. The method for Hg purification was the same as that already described[11]. The preparation of the solutions was made as described elsehwere[12]. Solutions of HCl with LiCl as supporting electrolyte in the concentration range of 2×10^{-3} M to 0·5 M at total ionic strength of 0·5 were employed. Solutions were either H_2- or N_2-saturated. These gases were purified by passing them through a dry, lubricant-free system, as described before[11]. Experiments were performed within the temperature range 25 to 55°C, both under galvanostatic and potentiostatic conditions. The cathodic overvoltage decay was recorded with conventional procedure. The electrode capacitance measurements were performed on a *dme* using an improved version of Grahame's method, as described previously[11].

In most of the runs the rapid-polarization galvanostatic technique was used and owing to the instability of the points the applied potential was changed in a decreasing direction[13]. Faster and better readings were obtained in this fashion. The average currents were between 5×10^{-5} to 1×10^{-2} A, the upper limit being safe against the occurrence of undesirable side reactions in the HCl–DMSO medium. Potentiostatic E/I curves were also recorded. The ohmic or pseudo-ohmic drops were measured by means of the well-known galvanostatic step method. The pseudo-ohmic resistance varied from one run to the other; it was between 8 and 15 ± 2 Ω.

RESULTS

The hydrogen gas yield

The yield of hydrogen gas was determined by weighing it as H_2O after its oxidation in a CuO furnace at 400°C. The H_2 gas was removed from the electrolysis cell by means of N_2 gas passed through for 24 h after current interruption. At 0·46 mA/cm², the constant-current hydrogen gas yield was 96·8 per cent. Thus, the over-all reaction can be expressed as

$$2\,H^+(\text{solv}) + 2\,e \longrightarrow H_2(g). \qquad (1)$$
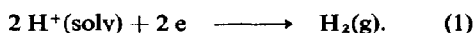
The rest potential

The initial rest potential, E_r^i, was measured against a sce at different HCl concentrations and temperature (Table 1). The final rest potentials obtained

Table 1. Rest Potentials

c_{HCl} M	c_{LiCl} M	Temp °C	E_r^i V	E_r^f V
2×10^{-3}	0·5	25	−0·362	—
5×10^{-3}	0·5	25	−0·385	—
		35	−0·375	—
		45	−0·375	−0·385
2×10^{-2}	0·5	28	−0·382	−0·400
		37	−0·385	−0·390
		47	−0·367	−0·375
0·1	0·4	25	−0·368	—
		25	−0·395	−0·400
		25	−0·370	−0·380
		35	−0·375	—
		45	−0·400	—
0·5	—	25	−0·318	−0·345
		25	−0·335	—
		25	−0·323	—
		25	−0·310	—

after electrolysis, E_r^f, are also assembled in the Table. These are slightly more negative than E_r^i. Except for the solution which contained no LiCl, no particular concentration effects on E_r^i and E_r^f were noticed.

The current/voltage curves

Figure 1 shows one potentiostatic and one galvanostatic E/I curve obtained with a 0·5 M HCl solution at 25°C. The former exhibits at low potentials a cathodic current maximum of the order of 450 μA. In the potential range from −0·40 to −0·60 V, a constant current of ca 100 μA is observed. At potentials more cathodic than −0·65 V, a Tafel region is obtained involving an initial slope close to $2·3(2RT/F)$. At higher current the slope tends to increase because of pseudo-ohmic polarization. The
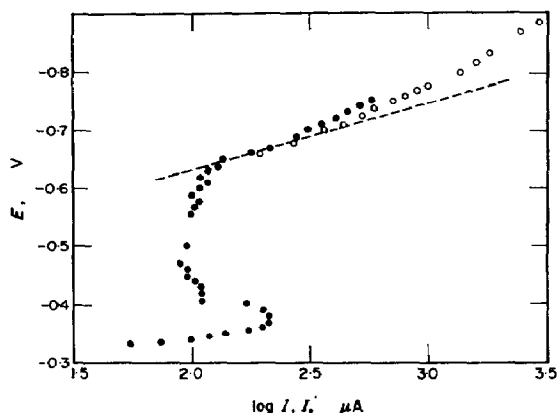

Fig. 1. Semilogarithmic plots of E/I curves without the correction for the pseudo-ohmic polarisation. Dotted line corresponds to a slope $2·3(2RT/F)$. 0·5 M HCl; 25°C. ●, potentiostatic, $E_{rest} = -0·323$ V (sce); ○, galvanostatic, $E_{rest} = -0·310$ V (sce).

galvanostatic E/I curve reproduces the Tafel line region of the potentiostatic curve.

The maximum cathodic current at low cathode potentials has been also recorded in polarographic experiments with HCl–DMSO solutions containing LiCl as supporting electrolyte (Fig. 2).
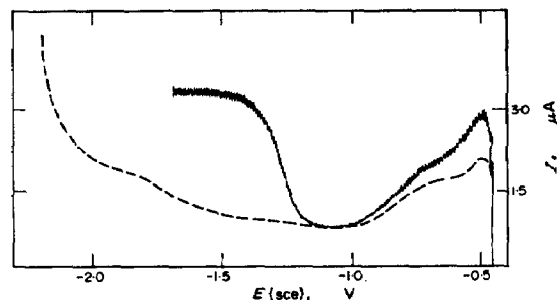

Fig. 2. Polarogram of a 2×10^{-3} M HCl + 0·5 M KClO₄ solution at 18°C. Dotted line corresponds to a blank at 35°C. t (open circuit), 2·06 s; m, $3·3 \times 10^{-3}$ g/s; dE/dt, 0·05 V/min.

Galvanostatic cathodic E/I curves recorded at constant ionic strength and different hydrogen-ion concentration and temperature are plotted as $E/\log I$ relationships in Fig. 3, after correction for the pseudo-ohmic polarization. Tafel slopes obtained from the E/I plots are assembled in Table 2. They are close to $2·3(2RT/F)$, as in the cases previously described. The i_0 values referred in the Table are extrapolated at the rest potentials. Those potentials, as reported further on, are quite close to the pzc of the Hg electrode in these solutions. Unfortunately the complex and rather irreproducible initial behaviour of the E/I curves at low cathode potentials makes it

Table 2. Kinetic parameters derived from current/potential curves

c_{HCl} M	c_{LiCl} M	Temp °C	$(\Delta E/\Delta \log i)_c$* V	$2\cdot3(2RT/F)$ V	$\log i_0$ (i_0 in A/cm²)	$\Delta H^*_{\eta=0}$ kcal/mole
$0\cdot5 \times 10^{-2}$	0·5	25	0·112	0·118	−9·923	18·7
		35	0·126	0·122	−9·473	
		45	0·135	0·126	−9·148	
$0\cdot2 \times 10^{-1}$	0·5	28	0·121	0·119	−9·513	12·8
		37	0·117	0·123	−9·293	
		47	0·114	0·127	−8·993	
0·1	0·4	25	0·112	0·118	−8·723	16·0
		35	0·108	0·122	−8·373	
		45	0·103	0·126	−8·073	
0·5		25	0·130	0·118	−7·500	—

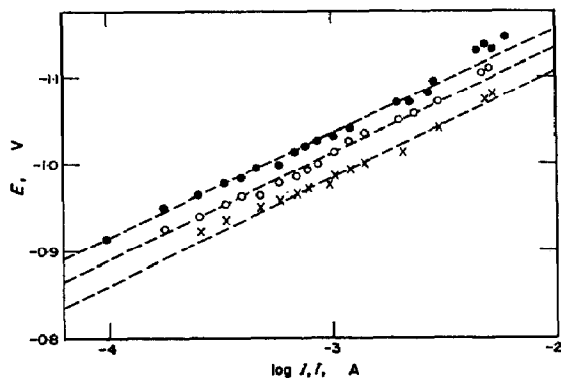* The estimated error for the Tafel slope is about 15 per cent.

Fig. 3. Semilogarithmic plots of galvanostatic cathodic E/I curves, after correction for the pseudo-ohmic polarisation.
0·1 M HCl + 0·4 M LiCl; ●, 25°C; ○, 35°C; ×, 45°C.

impossible to obtain experimental information for the calculation of the stoichiometric number.

The polarization limits of LiCl solutions, as determined polarographically, are shown in Fig. 2. The anodic limit is +0·40 V(sce) and the cathodic
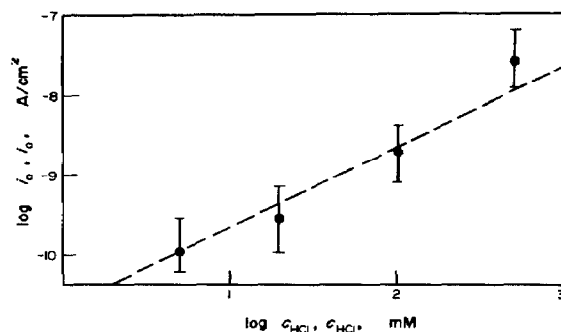

Fig. 4. Log–log plot of i_0 vs HCl concentration. Dotted line slope is unity.

is −1·90 V(sce). The slight inflexion of the E/I polarogram may be due to water reaction[14].

The i_0 obtained at constant ionic strength exhibits a first-order dependence on the hydrogen chloride concentration, as seen in Fig. 4.

Non-steady measurements

Semilogarithmic plots of cathode potential decay at current interruptions are shown in Figs. 5 and 6 for different experimental conditions. The plots exhibit a reasonable straight-line portion covering the potential range corresponding to the the Tafel-line region of the $E/\log I$ plots. Kinetic parameters derived from these decay curves are indicated in Table 3. E_1 is the potential at the current interruption, $(dE/d \log t)$ is the decay slope in the linear portion of the semilogarithmic plot and C is the apparent electrode differential capacitance at E_1. The dependence of C on the electrode potential was evaluated from the analysis of the whole decay curve
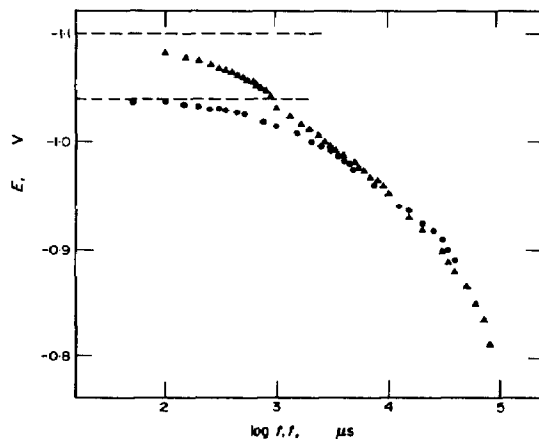

Fig. 5. Semilogarithmic plots of cathodic overvoltage decay at current interruption.
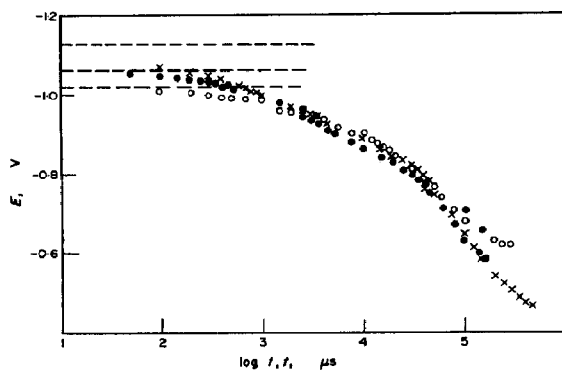2×10^{-2} M HCl + 0·5 M LiCl; 25°C.

Fig. 6. Semilogarithmic plots of cathodic overvoltage
decay at current interruption.
0·1 M HCl + 0·4 M LiCl.

Table 3. Parameters derived from cathodic potential-
decay curves at 25°C

c_{HCl}* M	$(E - E_r^1)$ V	$(\partial E/\partial \log t)$ V	C $\mu F/cm^2$
0·02	−0·658	0·089	6·68
0·02	−0·688	0·091	8·52
0·02	−0·718	0·089	3·20
0·1	−0·620	0·130	6·68
0·1	−0·635	0·130	8·06
0·1	−0·675	0·125	5·82
0·1	−0·735	0·117	3·15

* All solutions $\mu = 0·5$ with LiCl.

according to $C = i_t/(dE/dt)_t$, where i_t is the current
density at time t. As seen in Fig. 7, in the potential
range −0·8 to −1·07 V(sce) the apparent electrode
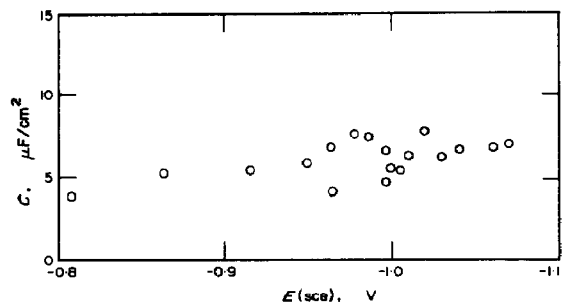capacitance fluctuates about an average constant
value.

Fig. 7. Electrode capacitance (as calculated from the
analysis of the whole decay curve) vs electrode potential.
0·1 M HCl + 0·4 M LiCl; 25°C.

Electrode-capacitance measurements

Figure 8 shows the C/potential curve of the Hg
electrode in 0·5 M LiCl solutions at 25°C determined
by the *dme* method. The potential of the electro-
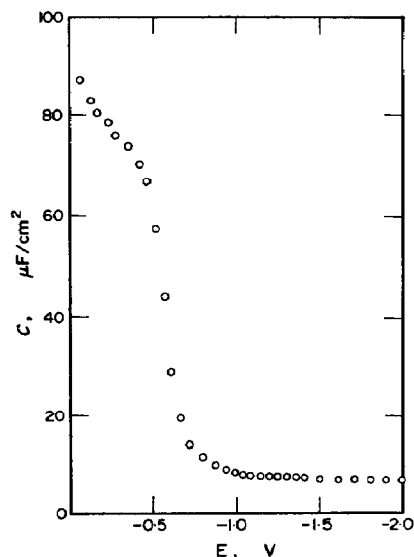capillary maximum is also indicated in the figure.

Fig. 8. Electrode capacitance measured by the im-
pedance-bridge method on a dme.
0·5 M LiCl, 25°C; $E_z = -0·4798$ V(0·1 Nce).

The zero-charge parameter was obtained by the
mercury-jet method indicated by Grahame[15].
At high chloride-ion concentration, ca 0·5 M, a
reversible potential is set up near the measured *pzc*
(*viz* −0·4 V vs 0·1 N calomel electrode), which is
probably due to an anodic dissolution of the Hg
electrode.

DISCUSSION

Let us first consider the possible structure of the
electrical double layer in the potential region where
the cathodic evolution of hydrogen from solvated
hydrogen ion occurs. The potential dependence of
the electrode differential capacitance resembles, as
could be expected, that of NH_4Cl solutions and
KBr solutions in DMSO, the values being nearly
coincident with those reported by Payne.[16] The
different experimental data on electrode capacitance
already mentioned, particularly the low values of C
and their independence of potential in the hydrogen-
ion-discharge region, supports the idea of a rather
simple double-layer structure at the reaction inter-
face, at least not affected by appreciable accumula-
tion of reaction intermediates. Furthermore, this
also explains in a simple way the reasonable coin-
cidence of the Tafel slopes obtained from the rapid
$E/\log I$ curves with the decay slopes of the linear
portion of the $E/\log t$ plots.

The kinetic parameters obtained for the hydro-
gen-ion discharge on Hg electrodes employing
HCl–LiCl–DMSO solutions indicate a slow reac-
tion rate, as deduced from the exchange *cd* defined
with respect to the *pzc*. This behaviour is consistent
with that of Hg electrodes in aqueous solutions.

Therefore the Tafel slope is probably related to the initial electron-transfer step involving the hydrogen-ion-discharge as rate-determining, on condition that the degree of surface coverage by hydrogen atoms is practically zero. The second step should occur under quasi-equilibrium conditions, and it may be either the chemical desorption of hydrogen atoms yielding hydrogen molecules or their electrodic desorption. In this case the transfer coefficient, α, is simply equal to the symmetry factor β, ($\alpha = \beta = 0.5$). The rate equation is then

$$i = 2Fk_1 c_{H^+} \exp\left[\frac{-F(E - E_z)}{2RT}\right], \qquad (2)$$

where k_1 is the formal specific rate constant for the initial electron transfer step, c_{H^+} is the hydrogen-ion concentration at the reaction interface, E is the electrode potential and E_z is the potential of zero charge.

In the presence of the supporting electrolyte, the potential drop from the outer Helmholtz plane to the solution will tend to zero; therefore, if the reference potential (either the *pzc* or the initial rest potential) does not depend on the concentration of hydrogen ion, (2) implies the first-order dependence found between i_0 and c_{H^+}, instead of the one-half order expected for the corresponding reaction mechanism in water, the hydrogen electrode being taken as reference[17]. As a consequence of the above-mentioned assumptions, results obtained for HCl–DMSO solutions, in the absence of supporting electrolyte, although included in the same plot (Fig. 4) are not directly comparable to the other results. The thermodynamics of HCl and LiCl solutions, as far as the corresponding activity coefficients are concerned, are fairly similar,[12, 18, 19] although no sound arguments are available to decide about structural changes in the DMSO electrical double layer when passing from Li^+ ion to H^+ (solvated) ion.

The experimental activation energy, at $(E - E_{zpc}) = 0$, should in consequence be related to the activation energy of the rate-determining step. Its average value, calculated from the temperature dependence of the i_0 values reported in Table 2, is 15.8 ± 3 kcal/mole. This figure must increase with cathodic overvoltage in the way predicted by (2). However, as the error of the activation energy is rather large, no additional kinetic information can be derived from it.

In conclusion, the mechanism for the hydrogen-evolution reaction on Hg in HCl–DMSO solutions is probably related to an initial proton-discharge rate-determining step followed by electrodic desorption. Formally it corresponds to the reaction mechanism established for the reaction on Hg cathodes in acid aqueous solutions.

REFERENCES

1. K. Vetter, *Electrochemical Kinetics*, p. 538. Academic Press, New York (1967).
2. I. M. Kolthoff and T. B. Reddy, *J. electrochem. Soc.* **108**, 980 (1961).
3. C. Papon and J. Jacq, *Bull. Soc. chim. Fr.* 13 (1965).
4. J. Courtot-Coupez and M. Le Démézet, *Bull. Soc. chim. Fr.* 4744 (1967).
5. J. A. Olabe and A. J. Arvía, *Electrochim. Acta* **14**, 785 (1969).
6. J. A. Olabe and A. J. Arvía. *Electrochim. Acta* **15**, 1685 (1970).
7. D. Posadas, J. J. Podestá and A. J. Arvía, *Electrochim. Acta* **15**, 1225 (1970).
8. A. Delgado, D. Posadas and A. J. Arvía, *Electrochim. Acta* in press.
9. A. de Béthune, *J. Am. chem. Soc.* **71**, 1556 (1949).
10. P. Delahay, *New Instrumental Methods in Electrochemistry*, Interscience, New York (1966).
11. G. Paus and D. Posadas, *An. Soc. cient. Argent.*, **192**, 239 (1971).
12. J. A. Bolzan and A. J. Arvía, *Electrochim. Acta* **15**, 39 (1970).
13. J. O'M Bockris, R. Parsons and H. Rosenberg, *Trans. Faraday Soc.* **47**, 766 (1951).
14. V. Gutmann and G. Schoeber, *Z. anal. Chem.* **5**, 339 (1959).
15. D. C. Grahame, M. Poth and J. Cummings, *J. Am. chem. Soc.* **74**, 4422 (1952).
16. R. Payne, *J. Am. chem. Soc.* **89**, 489 (1967).
17. B. E. Conway, *Theory and Principles of Electrode Process*. Ronald, New York (1965).
18. W. H. Smyrl and C. W. Tobias, *J. electrochem. Soc.* **115**, 33 (1968).
19. D. R. Cogley and J. N. Butler, *J. phys. Chem.* **72**, 1017 (1968).